molecules

MDPI

Article

Can the Fluxionality in Borospherene Influence the Confinement-Induced Bonding between Two Noble Gas Atoms?

Ranita Pal [1] and Pratim Kumar Chattaraj [2,*]

[1] Advanced Technology Development Centre, Indian Institute of Technology Kharagpur, Kharagpur 721302, India
[2] Department of Chemistry, Indian Institute of Technology Kharagpur, Kharagpur 721302, India
* Correspondence: pkc@chem.iitkgp.ac.in

Abstract: A density functional theory study is performed to determine the stability and bonding in the neon dimer inside the $B_{30}N_{30}$ fullerene cage, the fluxional B_{40} cage, and within non-fluxional cages such as $B_{12}N_{12}$ and C_{60}. The nature of bonding in the Ne_2 encapsulated B_{40} is compared with the that in other cages in an attempt to determine whether any possible alterations are brought about by the dynamical nature of the host cage apart from the associated confinement effects. The bonding analysis includes the natural bond order (NBO), Bader's Atoms-in-Molecules electron density analysis (AIM), and energy decomposition analysis (EDA), revealing the non-covalent nature of the interactions between the Ne atoms and that between the Ne and the cage atoms. The formation of all the Ne_2@cage systems is thermochemically unfavourable, the least being that for the $B_{30}N_{30}$ cage, which can easily be made favourable at lower temperatures. The Ne-Ne distance is lowest in the smallest cage and increases as the cage size increase due to steric relaxation experienced by the dimer. The dynamical picture of the systems is investigated by performing ab initio molecular dynamics simulations using the atom-centred density matrix propagation (ADMP) technique, which shows the nature of the movement of the dimer inside the cages, and by the fact that since it moves as a single entity, a weak bonding force holds them together, apart from their proven kinetic stability.

Keywords: fluxionality; encapsulation; borospherene; fullerene; noble gas

Citation: Pal, R.; Chattaraj, P.K. Can the Fluxionality in Borospherene Influence the Confinement-Induced Bonding between Two Noble Gas Atoms? *Molecules* **2022**, *27*, 8683. https://doi.org/10.3390/molecules27248683

Academic Editor: Ángel Martín Pendás

Received: 30 October 2022
Accepted: 4 December 2022
Published: 8 December 2022

1. Introduction

Encapsulation of noble gas (Ng) atoms and their dimers is widely studied in many caged systems in an attempt to understand the possible bonding between the so-called "inert" elements. Owing to their high and low IP and EA, respectively, noble gases tend to be chemically "inert: towards other elements unless they are subjected to a strong polarizing source that would facilitate a deformation in their otherwise rigid electron density to induce a donor–acceptor type of interaction. Noble gas dimers only have weak dispersive interactions within them. Confining them within molecular cages allows them to interact with the cage atoms as well as with each other. Although in most cases the complex formation is not thermochemically favourable, they have kinetic stability and hence do not disintegrate easily once formed. The most common caged compounds to form stable endohedral complexes with varied types of atoms and molecules are the carbon fullerene compounds. Confining noble gas atoms within neutral as well as cationic fullerene systems was experimentally performed using high-energy bimolecular collision reactions for the charged ones. For the neutral systems, generating C_{60} from graphite in a He atmosphere, using high temperatures to achieve the "window mechanism" where the Ng atoms are inserted via the formation of a temporary window by breaking one or more of the cage C-C bonds, was adopted. [1–14]. Later on, the insertion process involved the use of cationic Ng beams on the fullerene cage [15], "molecular surgery" [16,17], etc. The study of endohedral

metallofullerenes is also being explored in recent times [18]. Guest–host confined systems with a single Ng atom (He-X) [14] and with Ng dimers within the cavity of C_{60} have been reported both experimentally [19] as well as theoretically, along with that of several other small molecules such as HF, CO_2, H_2, H_2O, etc. [20–24]. Soon after the theoretical prediction of noble gas dimers trapped within fullerene [25], the experimental detection of $He_2@C_{70}$ and $Ne_2@C_{70}$ was reported through NMR and mass spectrometry [26,27]. The confined Ng atoms within the fullerene cages exhibit a van der Waals type of interaction between them to attain stability in most cases. There exists no genuine chemical bond between the guest atoms and the cage C atoms. However, the presence of a "chemical bond" between two Xe atoms confined with the C_{60} cage is claimed by Krapp and Frenking [20]. Other than fullerenes, noble gas confinement within cages with much smaller cavities such as $C_{10}H_{16}$, $C_{20}H_{20}$ and $Mo_6Cl_8F_6$ [28–31], along with those within smaller BN-fullerenes, such as $B_{12}N_{12}$ and $B_{16}N_{16}$, [32] is also performed to study their viability and stability.

Pure boron cages are also explored in this regard. Among them, the borospherene, B_{40} cage, shows some interesting features regarding its dynamical behaviour. It contains four numbers of heptagonal and two hexagonal holes, with a HOMO-LUMO energy gap comparable to that of C_{60}. A molecular dynamics study on the molecule reveals the dynamical behaviour of the cluster arising from a continuous interconversion between the two types of holes (B_6 and B_7) [33]. The B_{40} molecule has been previously used to trap Ng atoms, and the dynamical behaviour of the $Ng@B_{40}$ system is similar to that of the bare cage [34]. The C_{60}, on the other hand, cannot undergo rapid interconversion among its isomers due to its rigid σ-framework. It contains 12 5-C and 20 6-C rings [35]. Previously, it was proposed that any B, N doped structures of fullerene should not have any B-B or N-N bonds. This required the B, N doped structure of C_{60} to have one C atom in all the five-membered rings, thus producing $C_{12}B_{24}N_{24}$ [36]. However, studies on the $B_{30}N_{30}$ ring show that it forms a stable structure, and it was also hypothesized that it can be easily synthesized from borazine [37]. We have encapsulated neon dimers within this cage to study the stability of the resulting complex and the bonding situation therein. The nature of bonding in the noble-gas-encapsulated borospherene is also investigated and compared with those of $B_{12}N_{12}$, $B_{30}N_{30,}$ and C_{60} cages in an attempt to determine whether any possible alterations are brought about by the dynamical nature of the host cage apart from that arising out of confinement. Density functional theory-based computations are performed, and the bonding analysis includes the natural bond order (NBO) [38,39] Bader's Atoms-in-Molecules electron density analysis (AIM) [40], and energy decomposition analysis (EDA) [41–43]. The dynamical picture of the systems is investigated by performing ab initio molecular dynamics simulations using the atom-centred density matrix propagation (ADMP) [44–46] technique.

2. Methods and Computational Details

Geometry optimizations and frequency calculations for the B_{40}, $B_{12}N_{12}$, $Ne_2@B_{40,}$ and $Ne_2@B_{12}N_{12}$ systems are performed using the DFT functional, ωB97X-D [47] with 6-311G(d,p) [48,49] basis set, while those of the larger systems, $B_{30}N_{30}$, C_{60}, $Ne_2@B_{30}N_{30,}$ and $Ne_2@C_{60}$, are performed using the 6-31G [50,51] basis set with the same DFT functional. The dissociation energies calculated for the system use the following equation:

$$D_e = E_{Ne_2} + E_{cage} - E_{Ne_2@cage} \quad (1)$$

The energy corresponding to the distortion that the host undergoes due to the encapsulation of the guest molecules (E_{dist}) is calculated as follows:

$$E_{\text{dist}} = E_{expanded\ cage} - E_{cage} \quad (2)$$

where E_{dist} is obtained by removing the Ne_2 molecule and by evaluating single-point energy of the expanded cage. Basis set superposition error (BSSE) is corrected by using the counterpoise method [52].

The natural charge on the atoms and Wiberg bond index between two atoms are calculated using NBO 3.1 [38] at the ωB97X-D/6-311G (d,p) level of theory. Electron density analysis is performed using the Multiwfn software [53] to calculate the relevant topological descriptors. The energy decomposition analysis performed at B3LYP-D3(BJ)/TZ2P//ωB97X-D/6-311G(d,p) (for $Ne_2@B_{40}$ and $Ne_2@B_{12}N_{12}$) and B3LYP-D3(BJ)/TZ2P//ωB97X-D/6-31G (for $Ne_2@B_{30}N_{30}$ and $Ne_2@C_{60}$) levels uses the ADF 2014.01 software [54,55] to evaluate different types of interactions between the Ne_2 and the respective cages. The interaction energy between two relevant fragments is evaluated as the total of the Pauli repulsive interaction (ΔE_{Pauli}) and three attractive interaction energies, viz., electrostatic (ΔE_{elstat},), orbital (ΔE_{orb}), and dispersive (ΔE_{disp}) interactions. Lastly, atom-centered density matrix propagation (ADMP) is utilized to carry out the ab initio molecular dynamics simulation. All the above computations are executed using the Gaussian 16 [56] program package in the supercomputing facility, PARAM Shakti, at IIT Kharagpur.

3. Results and Discussion

3.1. Structure and Stability

The cages considered for encapsulating neon dimers are the fluxional B_{40}, the non-fluxional $B_{12}N_{12}$, and the fullerenes C_{60} and $B_{30}N_{30}$. The optimized geometries of the encapsulated cage systems are provided in Figure 1. The fluxional borospherene cage has a D_{2d} symmetry with an $^1A_1$ electronic state. The B_{40} cage has two six-membered and four seven-membered ring structures, the continuous interconversion among which causes its fluxional behaviour akin to that of a nanobubble. On encapsulation of Ne_2, two possible geometries can be obtained, one with a C_{2v} symmetry and the other with a D_{2d} symmetry, where the former is marginally more stable. The bond axis of Ne_2 is oriented along the imaginary line connecting the midpoints of the two opposing B_7 rings in the former case and the B_6 rings in the latter case. The formation of both of these $Ne_2@B_{40}$ systems is thermochemically unfavourable (see Table 1); however, once formed, they have kinetic activation barriers high enough to protect from their spontaneous dissociation (~67.5 kcal mol^{-1} at ωB97X-D/def2-TZVP//ωB97X-D/def2-SVP level) [34]. The distance between the Ne atoms within the cavity reduces from 3.061 to 1.913 Å and to 1.877 Å in the C_{2v} and D_{2d} isomers, respectively. The distortion undergone by the host cage as a result of confining the Ne dimers within it is calculated as 6.395 and 8.106 kcal mol^{-1} for the C_{2v} and D_{2d} isomers, respectively.

Table 1. Zero-point (ZPE) corrected dissociation energy (D_0), both ZPE and BSSE corrected dissociation energy ($D_0{}^{BSSE}$), entropy change (ΔS) and free energy change (ΔG) for the dissociation processes, $Ne_2@cage \rightarrow Ne_2 + cage$, and $Ne_2@cage \rightarrow Ne + Ne@cage$ along with the distortion energy (E_{dist}) calculated as Equation (2). The energy values are provided in kcal mol^{-1} and the entropy change in kcal mol^{-1} K^{-1}.

Systems	E_{dist}	Processes	D_0	$D_0{}^{BSSE}$	ΔS	ΔG
$Ne_2@B_{40}$ (C_{2v})	6.395	$Ne_2@B_{40} \rightarrow Ne_2 + B_{40}$	−70.5	−81.5	0.048	−83.5
		$Ne_2@B_{40} \rightarrow Ne + Ne@B_{40}$	−69.3	−80.3	0.030	−77.4
$Ne_2@B_{40}$ (D_{2d})	8.106	$Ne_2@B_{40} \rightarrow Ne_2 + B_{40}$	−79.4	−90.6	0.049	−92.7
		$Ne_2@B_{40} \rightarrow Ne + Ne@B_{40}$	−78.1	−89.4	0.031	−86.5
$Ne_2@B_{12}N_{12}$	84.687	$Ne_2@B_{12}N_{12} \rightarrow Ne_2 + B_{12}N_{12}$	−449.8	−462.2	0.047	−462.7
		$Ne_2@B_{12}N_{12} \rightarrow Ne + Ne@B_{12}N_{12}$	−352.1	−364.5	0.026	−359.7
$Ne_2@B_{30}N_{30}$	0.604	$Ne_2@B_{30}N_{30} \rightarrow Ne_2 + B_{30}N_{30}$	5.3	−11.4	0.035	−5.1
		$Ne_2@B_{30}N_{30} \rightarrow Ne + Ne@B_{30}N_{30}$	−6.7	−23.5	0.030	−15.1
$Ne_2@C_{60}$	0.983	$Ne_2@C_{60} \rightarrow Ne_2 + C_{60}$	−6.9	−19.4	0.040	−31.0
		$Ne_2@C_{60} \rightarrow Ne + Ne@C_{60}$	−13.5	−26.0	0.033	−35.1

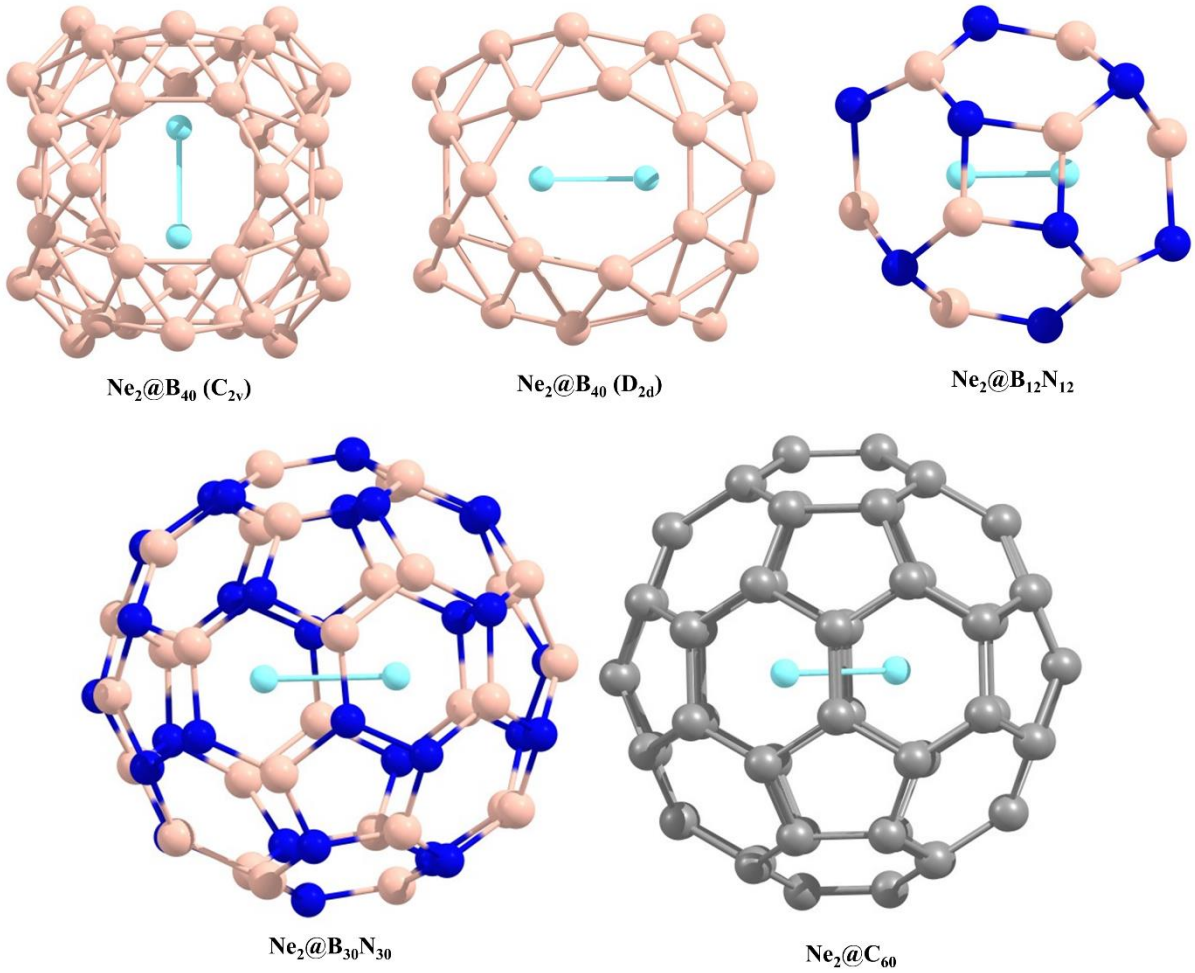

Figure 1. Optimized geometries of the Ne_2-encapsulated cages. The boron, carbon, nitrogen, and neon atoms are indicated by light pink, grey, dark blue, and sky blue colours, respectively.

The $B_{30}N_{30}$ cage is a BN analogue of the C_{60} fullerene. Out of the three possible geometries, as reported by Yin et al. [57], we have selected the one with the minimum energy where the cage contains six N-N bonds. It primarily differs from carbon fullerene in the fact that, unlike C_{60}, it has non-uniform diameters of the rings throughout the cage and is slightly larger than C_{60}. The encapsulation of Ne_2 within this cage is marginally unfavourable at room temperature (ΔG for the dissociation process is -5.073 kcal mol^{-1}), which indicates that at slightly lower temperatures, its formation will be thermochemically feasible. The interatomic distance between the Ne atoms is found to be 2.130 Å, which is relatively larger than that in the B_{40} cage owing to the availability of ample space within the $B_{30}N_{30}$ cage. For this reason, the encapsulation of dimers of higher noble gas atoms is also viable without distorting the cage, much like the case in its carbon analogue. The $B_{12}N_{12}$ cage, on the other hand, has a much smaller cavity with four- and six-membered rings. On Ne_2 encapsulation, it becomes distorted to a much higher extent than all the other cages in consideration in this study (see Table 1). The Ne-Ne distance is also much lower (1.602 Å) due to the higher confinement effect of the small host cage. All attempts of inserting Ar_2 within the cage failed due to insufficient space within the cage. Insertion of Ng dimers within C_{60} has been reported earlier. It can accommodate dimers of higher noble gas elements as well with distortions increasing with increasing size of the Ng atoms. In the case of $Ne_2@C_{60}$, the internuclear distance between the Ne atoms is 2.050 Å. Several geometries with different point group symmetries are possible for this system, which are energetically close to each other. This occurs due to the precessional motion of the dimer inside the cage [58].

Table 1 presents the zero-point corrected dissociation energy (ZPE, D_0), both ZPE and BSSE corrected dissociation energy ($D_0{}^{BSSE}$), entropy change (ΔS) and free energy change (ΔG) for the dissociation processes, Ne_2@cage → Ne_2 + cage, and Ne_2@cage → Ne + Ne@cage. The $D_0{}^{BSSE}$ has higher negative values than the corresponding D_0 values. From the distortion and dissociation energy values, it is clear that the amount of destabilization to the cage caused by the Ne_2 encapsulation decreases with their increasing cavity size. Although the $Ne_2@B_{30}N_{30}$ cage showed a small positive dissociation energy, the introduction of the BSSE correction produced a small negative dissociation energy. Among all the cages considered, the encapsulation of Ne_2 within the $B_{30}N_{30}$ cage seems to be the most likely to be made favourable at lower temperatures. To determine the reaction energy of the process, 2Ne + cage → [Ne_2@cage] (where the third brackets indicate that the system is frozen in that geometry), we need to calculate the energies step by step: first, the energy required to bring the two Ne atoms to their equilibrium distance within the cages, i.e., 2Ne → [Ne_2], where [Ne_2] indicates the frozen geometry of Ne_2 as obtained within the respective cages; second, the energy [E_{dist}] involved in the distortion of the cages in their equilibrium state to the geometry they attain after encapsulating the Ne_2, i.e., cage → [cage]; finally, the interaction energy between the frozen dimer and cage, i.e., [Ne_2] + [cage] → [Ne_2@cage]. The aforementioned energies are tabulated in Table 2.

Table 2. Reaction energies calculated for all Ne_2@cage systems.

Processes	Reactions	E_R (kcal mol^{-1})
2Ne → [Ne_2]	2Ne → $[Ne_2]_{in\ [Ne_2@B_{40}]\ (C_{2v})}$	12.3
	2Ne → $[Ne_2]_{in\ [Ne_2@B_{40}]\ (D_{2d})}$	14.7
	2Ne → $[Ne_2]_{in\ [Ne_2@B_{12}N_{12}]}$	54.8
	2Ne → $[Ne_2]_{in\ [Ne_2@B_{30}N_{30}]}$	3.7
	2Ne → $[Ne_2]_{in\ [Ne_2@C_{60}]}$	5.8
cage → [cage]	B_{40} → $[B_{40}]_{in\ [Ne_2@B_{40}]\ (C_{2v})}$	6.4
	B_{40} → $[B_{40}]_{in\ [Ne_2@B_{40}]\ (D_{2d})}$	8.1
	$B_{12}N_{12}$ → $[B_{12}N_{12}]_{in\ [Ne_2@B_{12}N_{12}]}$	84.7
	$B_{30}N_{30}$ → $[B_{30}N_{30}]_{in\ [Ne_2@B_{30}N_{30}]}$	0.6
	C_{60} → $[C_{60}]_{in\ [Ne_2@C_{60}]}$	1.0
[Ne_2] + [cage] → [Ne_2@cage]	[Ne_2] + [B_{40}] → [$Ne_2@B_{40}$] (C_{2v})	50.3
	[Ne_2] + [B_{40}] → [$Ne_2@B_{40}$] (D_{2d})	55.1
	[Ne_2] + [$B_{12}N_{12}$] → [$Ne_2@B_{12}N_{12}$]	312.8
	[Ne_2] + [$B_{30}N_{30}$] → [$Ne_2@B_{30}N_{30}$]	−10.9
	[Ne_2] + [C_{60}] → [$Ne_2@C_{60}$]	11.5
2Ne + cage → [Ne_2@cage]	2Ne + B_{40} → [$Ne_2@B_{40}$] (C_{2v})	69.0
	2Ne + B_{40} → [$Ne_2@B_{40}$] (D_{2d})	77.8
	2Ne + $B_{12}N_{12}$ → [$Ne_2@B_{12}N_{12}$]	452.2
	2Ne + $B_{30}N_{30}$ → [$Ne_2@B_{30}N_{30}$]	−6.6
	2Ne + C_{60} → [$Ne_2@C_{60}$]	18.3

3.2. Bonding

The interactions between the two Ne atoms inside the cages are investigated in terms of NBO, AIM, and EDA. The internuclear bond distances of the free Ne dimer is reported to be 3.091 Å [59], and the atoms are bound to each other with weak van der Waals forces of attraction. In the studied complexes, the Ne-Ne distances are 1.913 and 1.877 Å in the C_{2v} and D_{2d} isomers of $Ne_2@B_{40}$, and 1.602, 2.130, and 2.050 Å in $Ne_2@B_{12}N_{12}$, $Ne_2@B_{30}N_{30}$, and $Ne_2@C_{60}$ systems, respectively. There is clearly an increase in the interatomic interaction, the extent of which is discussed to determine whether the resulting situation can be considered a genuine chemical bond.

The natural charges on the Ne atoms calculated within the cage systems are much higher in the smaller $B_{12}N_{12}$ (q_{Ne} = 0.137 |e|) than in the larger cages (q_{Ne} = 0.047 |e|, 0.042 |e|, and 0.010 |e| in B_{40}, $B_{30}N_{30}$, and C_{60}, respectively) (Table 3). The charge on

the cage atoms of the bare host in $B_{12}N_{12}$ is 1.164 |e| (positive on the B and negative on the N atoms, respectively), which increases after encapsulating the Ne_2. q_B and q_N ranges within 1.221–1.301 |e| and −1.252–−1.272 |e|, respectively, in the $Ne_2@B_{12}N_{12}$ system. The B atoms in the fluxional B_{40} cage have varied charges. In each of the two B_6 rings, two opposing B atoms have $q_B = -0.210$ |e| while the others have $q_B = 0.118$ |e|, whereas the charges on the rest of the B atoms constituting the B_7 rings range within −0.035–0.121 |e|. In the case of $B_{30}N_{30}$ and C_{60}, very little to no change is observed in the natural charges on the cage atoms. Positive charges on the Ne atoms on encapsulation indicate that a partial charge cloud transfer occurs from them to the caged atoms. Wiberg bond indices calculated for the interaction between the two Ne atoms reveal very low values (ranging within 0.0003−0.0004), which are just marginally higher than that in the free Ne dimer (0.0002). WBI values in such low ranges reveal the presence of a van der Waals type of interaction and the absence of any covalent interactions. The total WBI values for the Ne atoms are 0.274, 0.102 (and 0.100), 0.0837, and 0.0231 in $Ne_2@B_{12}N_{12}$, C_{2v} (and D_{2d}) isomer of $Ne_2@B_{40}$, $Ne_2@B_{30}N_{30}$, and $Ne_2@C_{60}$, respectively. The higher the total WBI values, the higher the extent of interactions between the Ne and the respective cage atoms.

Table 3. Natural charges on the encapsulated Ne atoms, the WBI values between two Ne atoms, and the total WBI value of Ne atoms.

Systems	$q_{Ne(1)}$	$q_{Ne(2)}$	$WBI_{Ne\text{-}Ne}$	Total WBI_{Ne}
$Ne_2@B_{12}N_{12}$	0.137	0.137	0.0027	0.2736
$Ne_2@B_{40}$ (C_{2v})	0.047	0.047	0.0003	0.1015
$Ne_2@B_{40}$ (D_{2d})	0.046	0.046	0.0004	0.1001
$Ne_2@C_{60}$	0.010	0.010	0.0251	0.0231
$Ne_2@B_{30}N_{30}$	0.041	0.042	0.0003	0.0837

Bader once claimed that the presence of a bond path between two atoms in a molecule in its equilibrium state indicates that there exists a bond between the two [60]. This statement is quite controversial [61–66] and is proven not to be true in many cases. We, therefore, rely on the AIM topological analysis to determine the nature of the interaction, rather than claim the presence of a bond just based on the presence of a bond path. Figure 2 depicts the contour diagrams for the Laplacian of the electron density, $\nabla^2\rho(r_c)$, calculated for the Ne_2@cage systems. Ne-Ne bond paths are present in all the systems. Six numbers of Ne-N bond paths are detected in the $Ne_2@B_{12}N_{12}$ system, three Ne-N in $Ne_2@B_{30}N_{30}$, six and four Ne-B in the C_{2v} and D_{2d} isomers of $Ne_2@B_{40}$, respectively, and ten Ne-C in $Ne_2@C_{60}$ (see Figure 3). We are interested in the nature of interactions that exists between the two Ne atoms under confinement; thus, we have calculated the relevant topological descriptors, viz., electron density ($\rho(r_c)$), its Laplacian ($\nabla^2\rho(r_c)$), local potential, kinetic, and total energy densities ($V(r_c)$, $G(r_c)$, and $H(r_c)$), at the bond critical point (BCP) between the said atoms (Table 4). A positive value of the Laplacian of electron density indicates a depletion of the same, suggesting a noncovalent type of interaction. Although it is a necessary criterion, it is not a sufficient one. A positive value of the summation of the local energy densities (i.e., $H(r_c) = G(r_c) + V(r_c)$) along with positive $\nabla^2\rho(r_c)$ again points towards the nature of interaction being a non-covalent one [67]. In our cases, the $H(r_c)$ values are positive, but their values are so small (pretty close to zero) that they may change their sign in case we try different levels of theory and stroke all basis sets. It may be noted that for the dimers of larger Ng atoms such as Kr_2 and Ar_2, negative $H(r_c)$ values are obtained [34]. This means that a partial covalent bond exists in those two dimers. It follows the prognosis made by Linus Pauling that it is possible for heavier Ng atoms to form bonds owing to the fact that they contain loosely bound electrons [68]. The magnitude of $\rho(r_c)$, $\nabla^2\rho(r_c)$, $G(r_c)$ and $V(r_c)$ gradually decreases with the increase in the size of the cage, whereas $H(r_c)$ increases. The ratio $-G(r_c)/V(r_c) > 1$ in all the systems suggests a purely non-covalent interaction between the Ne atoms [69]. Again, the ratio of $G(r_c)$ to $\rho(r_c)$ provides an insight into the type of interaction: greater than 1 suggests the absence of any covalent interactions.

It has earlier been reported that in the $B_{12}N_{12}$ cage, some degree of covalent character can be induced between two He atoms [32,70]. Thus, this interesting behaviour of developing partial covalent bonding interaction can be investigated for heavier noble gas dimers as well by subjecting them to a similar degree of confinement. Of course, that would require increasing size of cages for increasing size of the noble gas elements.

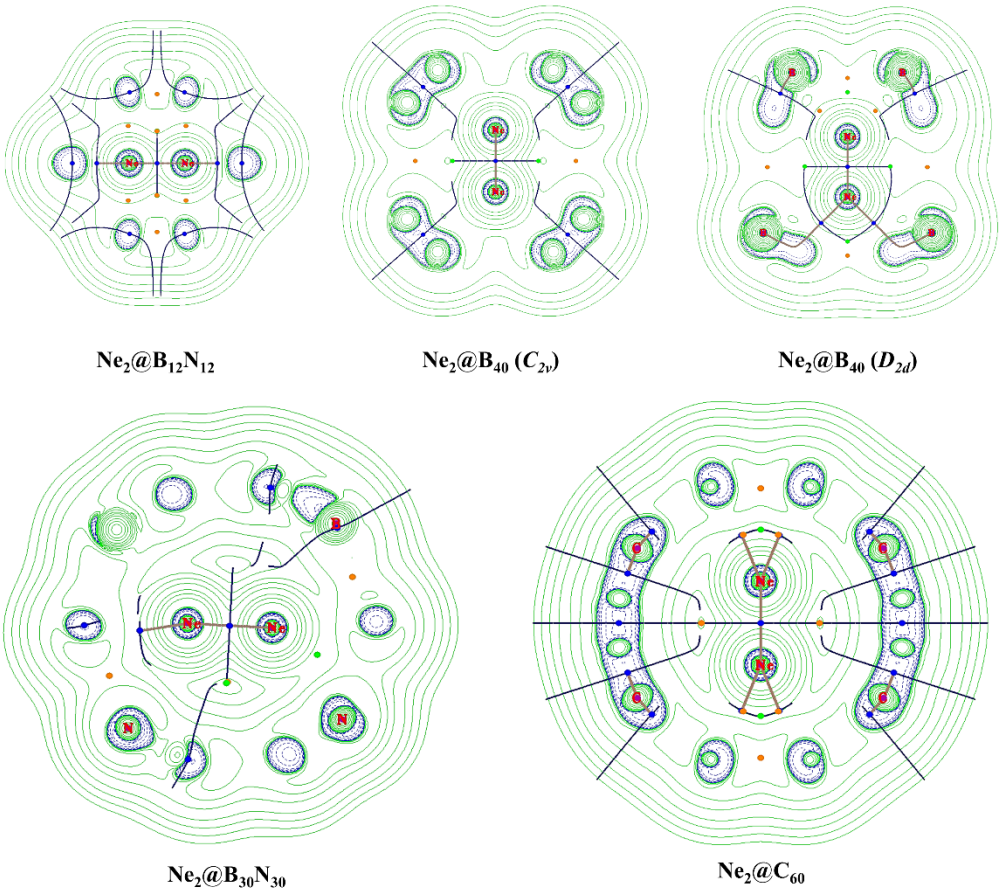

Figure 2. Contour diagrams of the Laplacian of the electron density of the Ne_2@cage systems. Green solid and blue dashed lines stand for positive and negative Laplacian, respectively.

The energy decomposition analysis is carried out considering Ne_2 and the cage as two separate fragments. The total interaction energies between the Ne dimer and the different cages are provided in Table 5 along with its components. The Pauli interaction energy is always positive, being repulsive in nature, and it decreases with increasing size of the host cage, highest and lowest corresponding to $B_{12}N_{12}$ and C_{60}, respectively. Among the attractive type of interaction energies, the electrostatic interaction dominates the other two. The percentage contribution to the net attractive energy of ΔE_{elstat}, ΔE_{orb}, and ΔE_{disp} are provided in parentheses, which clearly supports the above statement. In all the cases, the repulsive interaction is so high that it overcompensates all the attractive energies to result in an overall repulsive (positive) total interaction energy, the extent of which decreases with increasing cage size. Substantial orbital contribution is present in the case of Ne_2@$B_{12}N_{12}$, which decreases in the larger cages, whereas that of the dispersion interaction increases with cage size.

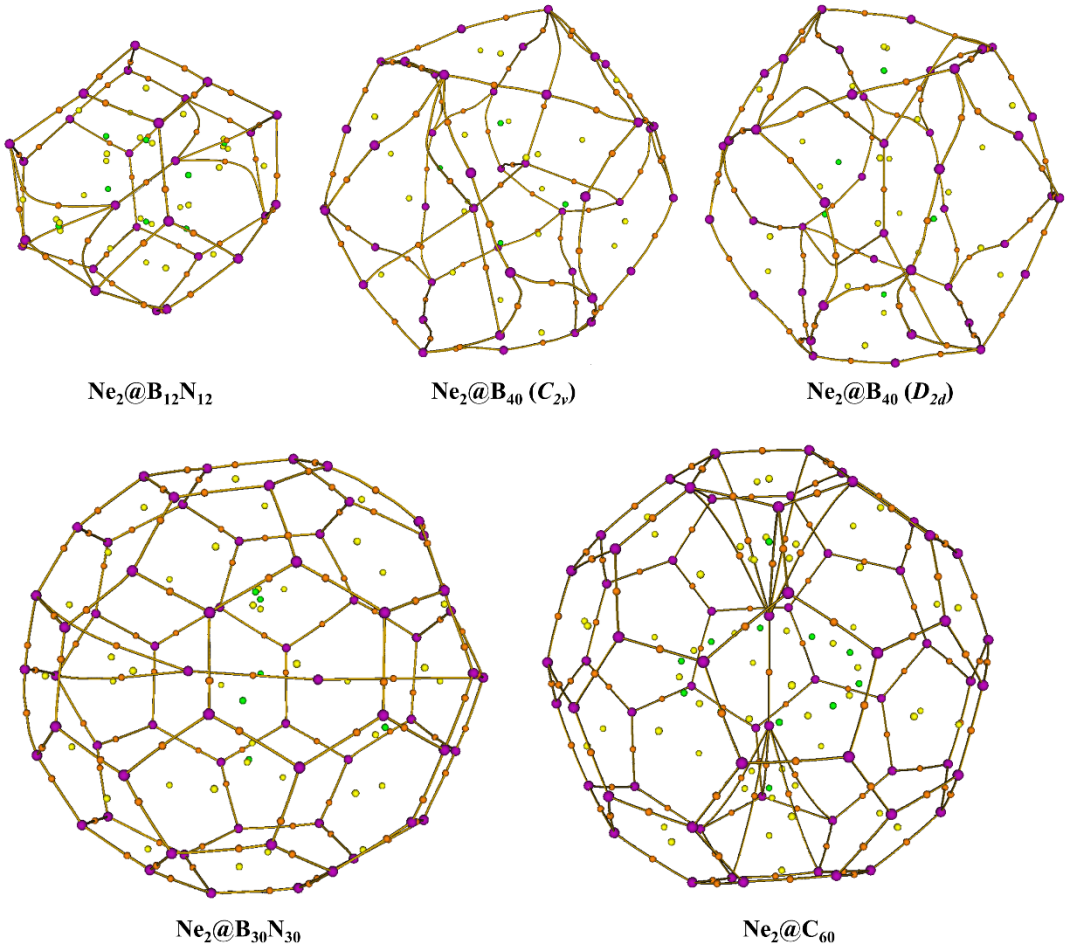

Figure 3. Molecular graphs generated for the Ne_2@cage systems showing the bond paths.

Table 4. Topological descriptors (a.u.) at the bond critical points (BCPs) between Ng atoms in Ne_2@cage systems.

Systems	ρ	$\nabla^2\rho(r_c)$	$G(r_c)$	$V(r_c)$	$-G(r_c)/V(r_c)$	$H(r_c)$	$G(r_c)/\rho(r_c)$	ELF
$Ne_2@B_{12}N_{12}$	0.130	1.255	0.313	−0.312	1.002	0.001	2.412	0.085
$Ne_2@B_{40}$ (C_{2v})	0.053	0.446	0.103	−0.095	1.089	0.008	1.933	0.042
$Ne_2@B_{40}$ (D_{2d})	0.059	0.497	0.116	−0.108	1.074	0.008	1.974	0.046
$Ne_2@C_{60}$	0.036	0.298	0.064	−0.054	1.184	0.010	1.810	0.029
$Ne_2@B_{30}N_{30}$	0.029	0.234	0.049	−0.040	1.237	0.009	1.716	0.024

Table 5. Total interaction energy values and components in kcal mol^{-1} obtained from EDA results Ne_2@cage systems using Ne_2 and the cage as the fragments.

Systems	ΔE_{int}	ΔE_{Pauli}	ΔE_{elstat}	ΔE_{orb}	ΔE_{disp}
$Ne_2@B_{12}N_{12}$	326.0	666.0	−249.4 (73.4)	−82.9 (24.4)	−7.7 (2.3)
$Ne_2@B_{40}$ (C_{2v})	59.0	132.9	−51.0 (69.0)	−11.7 (15.8)	−11.2 (15.2)
$Ne_2@B_{40}$ (D_{2d})	64.0	142.4	−54.5 (69.4)	−12.7 (16.2)	−11.3 (14.3)
$Ne_2@C_{60}$	7.6	35.0	−14.2 (51.6)	−2.2 (8.0)	−11.1 (40.4)
$Ne_2@B_{30}N_{30}$	4.2	28.1	−11.6 (48.4)	−2.0 (8.2)	−10.4 (43.4)

3.3. ADMP

The interconversion between the six- and seven-membered ring structures in the borospherene cage causes its fluxional behaviour, which has an activation free energy barrier of 14.3 kcal mol^{-1} [33]. Such transformation is possible owing to the appropriate

σ- and π- delocalization among the two possible isomers along with the corresponding transition state. The above transformation is observed in BOMD simulations performed at high temperatures of 1200 and 1500 K, which occur by the movement of one B atom during cage distortion from one of the heptagonal to the neighbouring hexagonal ring. Note that the higher temperatures are not indicative of the fact that the transformation occurs at those temperatures; this means that the higher temperatures help the system overcome the energy barrier within the very small simulation time window (in the order of *ps*). In realistic time scales, this can be observed at far lower temperatures. Upon encapsulating the noble gas monomer, no significant change is observed in the dynamical behaviour of the cage. ADMP simulations performed for the C_{2v} isomer of the dimer-encapsulated B_{40} at 400 K for a runtime of 500 fs show that the dimer undergoes slight precessional motion along the axis joining the centres of the two opposing heptagonal rings. The interconversions between the B_6 and B_7 rings are also observed (see simulation Video S1). Due to the smaller cavity size in $B_{12}N_{12}$, such movement of the guest molecule is restricted. Despite the larger sizes of the $B_{30}N_{30}$ and C_{60} cages, the Ne_2 inside their cavities does not move separately, but as a single entity, proving the existence of some bonding interaction, *albeit* weak, that holds them together. The dynamical study of the empty C_{60} cage investigated earlier at higher temperatures reported no fluxional behaviour because of the fact that the associated energy barrier for the transformation to its other isomeric forms is very high and is thermally forbidden by Woodward–Hoffmann rules [71].

4. Conclusions

The fluxional behaviour in any system arises due to the presence of low-lying energetically accessible isomers on the potential energy surface. If the energy barrier is low enough, the interconversion is easily observed. In the case of caged systems, this phenomenon can be monitored and utilized to influence the bonding, stability, and reactivity of any confined system or to catalyse a chemical reaction. The stability and bonding in the neon dimer are studied inside the fluxional B_{40} and some non-fluxional cages such as $B_{12}N_{12}$, $B_{30}N_{30}$, and C_{60} using a density functional theory approach. The formations of all the Ne_2@cage systems are thermochemically unfavourable, the least being that for the $B_{30}N_{30}$ cage, which can easily be made favourable at lower temperatures. The Ne-Ne distance is lowest in the smallest cage, and it increases as the cage size increases due to steric relaxation experienced by the dimer. NBO, AIM, and EDA reveal the non-covalent nature of the interaction between the Ne atoms and that between the Ne and the cage atoms. The dynamical study revealed the nature of movement of the dimer inside the cages and the fact that since it moves as a single entity, a weak bonding force holds them together. Since the fluxionality of the borospherene cage exists at a relatively higher temperature range, its effect on the bonding aspects is not very pronounced at lower temperatures. Additionally, the cage is too small to effectively host a chemical reaction without rupturing. Larger-sized fluxional cages may be inspected with different common reactions within to determine if a dynamic coupling exists between the confined reaction and the fluxional conversion (if so, whether both of them happen simultaneously or sequentially). The combined effect of confinement and fluxionality on certain chemical reactions may lead to some interesting and unusual results.

Supplementary Materials: The following supporting information can be downloaded at: https://www.mdpi.com/article/10.3390/molecules27248683/s1.

Author Contributions: Conceptualization, R.P. and P.K.C.; Data curation, R.P.; Formal analysis, R.P.; Funding acquisition, P.K.C.; Methodology, R.P.; Project administration, P.K.C.; Resources, P.K.C.; Supervision, P.K.C.; Validation, R.P. and P.K.C.; Writing—original draft, R.P.; Writing—review and editing, R.P. and P.K.C. All authors have read and agreed to the published version of the manuscript.

Funding: This research was funded by Department of Science and Technology (DST), New Delhi, grant number SR/S2/JCB-09/2009.

Institutional Review Board Statement: Not applicable.

Informed Consent Statement: Not applicable.

Data Availability Statement: Not applicable.

Acknowledgments: P.K.C. thanks the guest editors for kindly inviting him to contribute an article to the Special Issue of Molecules on, "New Boron Chemistry: Current Advances and Future Prospects". P.K.C. would also like to thank DST, New Delhi, for the J.C. Bose National Fellowship. R.P. thanks CSIR for her fellowship. We acknowledge National Supercomputing Mission (NSM) for providing computing resources of "PARAM Shakti" at IIT Kharagpur, which is implemented by C-DAC and is supported by the Ministry of Electronics and Information Technology and Department of Science and Technology (DST), Government of India.

Conflicts of Interest: The authors declare that they have no conflict of interest regarding the publication of this article, financial, and/or otherwise.

Sample Availability: Cartesian coordinates for the optimized geometries of the compounds are available from the authors on reasonable request.

References

1. Weiske, T.; Böhme, D.K.; Hrušák, J.; Krätschmer, W.; Schwarz, H. Endohedral cluster compounds: Inclusion of helium within C and C through collision experiments. *Angew. Chem. Int. Ed.* **1991**, *30*, 884–886. [CrossRef]
2. Weiske, T.; Hrušák, J.; Böhme, D.K.; Schwarz, H. Formation of endohedral carbon-cluster noble-gas compounds with high-energy bimolecular reactions: $C_{60}He^{n+}$ (n = 1, 2). *Chem. Phys. Lett.* **1991**, *186*, 459–462. [CrossRef]
3. Weiske, T.; Wong, T.; Krätschmer, W.; Terlouw, J.K.; Schwarz, H. The neutralization of HeC in the gas phase: Compelling evidence for the existence of an endohedral structure for He@C_{60}. Angew. *Chem. Int. Ed.* **1992**, *31*, 183–185. [CrossRef]
4. Weiske, T.; Böhme, D.K.; Schwarz, H. Injection of helium atoms into doubly and triply charged C_{60} cations. *J. Phys. Chem.* **1991**, *95*, 8451–8452. [CrossRef]
5. Ross, M.M.; Callahan, J.H. Formation and characterization of $C_{60}He^{+}$. *J. Phys. Chem.* **1991**, *95*, 5720–5723. [CrossRef]
6. Weiske, T.; Hrušák, J.; Bohme, D.K.; Schwarz, H. Endohedral fullerene-noble gas clusters formed with high-energy bimolecular reactions of Cx_{n+} (x = 60, 70; n = 1, 2, 3). *Helv. Chim. Acta* **1992**, *75*, 79–89. [CrossRef]
7. Wong, T.; Terlouw, J.K.; Weiske, T.; Schwarz, H. The neutralization—Reionization mass spectrum of C_{60}^{+}. *Int. J. Mass. Spectrom. Ion Process.* **1992**, *113*, R23–R29. [CrossRef]
8. Mowrey, R.C.; Ross, M.M.; Callahan, J.H. Molecular dynamics simulations and experimental studies of the formation of endohedral complexes of buckminsterfullerene. *J. Phys. Chem.* **1992**, *96*, 4755–4761. [CrossRef]
9. Wan, Z.; Christian, J.F.; Anderson, S.L. Ne^{+}+C_{60}: Collision energy and impact parameter dependence for endohedral complex formation, fragmentation, and charge transfer. *J. Chem. Phys.* **1992**, *96*, 3344–3347. [CrossRef]
10. Hrušák, J.; Böhme, D.K.; Weiske, T.; Schwarz, H. Ab initio MO calculation on the energy barrier for the penetration of a benzene ring by a helium atom. Model studies for the formation of endohedral He@C_{60}^{+} complexes by high-energy bimolecular reactions. *Chem. Phys. Lett.* **1992**, *193*, 97–100. [CrossRef]
11. Christian, J.F.; Wan, Z.; Anderson, S.L. Ne^{+}+C_{60} collisions: The dynamics of charge and energy transfer, fragmentation, and endohedral complex formation. *J. Chem. Phys.* **1993**, *99*, 3468–3479. [CrossRef]
12. Kleiser, R.; Sprang, H.; Furrer, S.; Campbell, E.E.B. He capture by negatively charged Buckminsterfullerene. *Zeitschrift für Physik D. At. Mol. Clust.* **1993**, *28*, 89–90. [CrossRef]
13. Saunders, M.; Jimenez-Vazquez, H.A.; Cross, R.J.; Poreda, R.J. Stable compounds of helium and neon: He@C_{60} and Ne@C_{60}. *Science* **1993**, *259*, 1428–1430. [CrossRef]
14. Saunders, M.; Jiménez-Vázquez, H.A.; James Cross, R.; Mroczkowski, S.; Gross, M.; Giblin, D.E.; Poreda, R.J. Incorporation of Helium, Neon, Argon, Krypton, and Xenon into Fullerenes Using High Pressure. *J. Am. Chem. Soc.* **1994**, *116*, 2193–2194. [CrossRef]
15. Shimshi, R.; Cross, R.J.; Saunders, M. Beam implantation: A new method for preparing cage molecules containing atoms at high incorporation levels. *J. Am. Chem. Soc.* **1997**, *119*, 1163–1164. [CrossRef]
16. Murata, M.; Murata, Y.; Komatsu, K. Surgery of fullerenes. *Chem. Commun.* **2008**, *46*, 6083–6094. [CrossRef] [PubMed]
17. Morinaka, Y.; Tanabe, F.; Murata, M.; Murata, Y.; Komatsu, K. Rational synthesis, enrichment, and ^{13}C NMR spectra of endohedral C_{60} and C_{70} encapsulating a helium atom. *Chem. Commun.* **2010**, *46*, 4532–4534. [CrossRef]
18. Liu, S.; Sun, S. Recent Progress in the Studies of Endohedral Metallofullerenes. *J. Organomet. Chem.* **2000**, *599*, 74–86. [CrossRef]
19. Sternfeld, T.; Hoffman, R.E.; Saunders, M.; Cross, R.J.; Syamala, M.S.; Rabinovitz, M. Two Helium Atoms inside Fullerenes: Probing the Internal Magnetic Field in C_{60}^{6-} and C_{70}^{6-}. *J. Am. Chem. Soc.* **2002**, *124*, 8786–8787. [CrossRef]
20. Krapp, A.; Frenking, G. Is This a Chemical Bond? A Theoretical Study of Ng_2@C_{60} (Ng = He, Ne, Ar, Kr, Xe). *Chem. Eur. J.* **2007**, *13*, 8256–8270. [CrossRef]

21. Straka, M.; Vaara, J. Density Functional Calculations Of 3 He Chemical Shift in Endohedral Helium Fullerenes: Neutral, Anionic, and Di-Helium Species. *J. Phys. Chem. A* **2006**, *110*, 12338–12341. [CrossRef] [PubMed]
22. Darzynkiewicz, R.B.; Scuseria, G.E. Noble Gas Endohedral Complexes of C_{60} Buckminsterfullerene. *J. Phys. Chem. A* **1998**, *102*, 3458. [CrossRef]
23. Yu Nikolaienko, T.; Kryachko, E.S.; Dolgonos, G.A. On the Existence of He-He Bond in the Endohedral Fullerene $He_2@C_{60}$. *J. Comput. Chem.* **2018**, *39*, 1090–1102. [CrossRef] [PubMed]
24. Yan, H.; Yu, S.; Wang, X.; He, Y.; Huang, W.; Yang, M. Dipole Polarizabilities of Noble Gas Endohedral Fullerenes. *Chem. Phys. Lett.* **2008**, *456*, 223–226. [CrossRef]
25. Giblin, D.E.; Gross, M.L.; Saunders, M.; Jiménez-Vázquez, H.; Cross, R.J. Incorporation of helium into endohedral complexes of C_{60} and C_{70} containing noble-gas atoms: A tandem mass spectrometry study. *J. Am. Chem. Soc.* **1997**, *119*, 9883–9890. [CrossRef]
26. Khong, A.; Jiménez-Vázquez, H.A.; Saunders, M.; Cross, R.J.; Laskin, J.; Peres, T.; Chava Lifshitz, R.S.; Amos, B.S. An NMR study of He_2 inside C_{70}. *J. Am. Chem. Soc.* **1998**, *120*, 6380–6383. [CrossRef]
27. Laskin, J.; Peres, T.; Lifshitz, C.; Saunders, M.; Cross, R.J.; Khong, A. An artificial molecule of Ne_2 inside C_{70}. *Chem. Phys. Lett.* **1998**, *285*, 7–9. [CrossRef]
28. Strenalyuk, T.; Haaland, A. Chemical Bonding in the Inclusion Complex of He in Adamantane (He@adam): The Origin of the Barrier to Dissociation. *Chem. Eur. J.* **2008**, *14*, 10223–10226. [CrossRef]
29. Cross, R.J.; Saunders, M.; Prinzbach, H. Putting Helium inside Dodecahedrane. *Org. Lett.* **1999**, *1*, 1479–1481. [CrossRef]
30. Jiménez-Vázquez, H.A.; Tamariz, J.; James Cross, R. Binding Energy in and Equilibrium Constant of Formation for the Dodecahedrane Compounds $He@C_{20}H_{20}$ and $Ne@C_{20}H_{20}$. *J. Phys. Chem. A* **2001**, *105*, 1315–1319. [CrossRef]
31. Zou, W.; Liu, Y.; Liu, W.; Wang, T.; Boggs, J.E. He@Mo6Cl8F6: A Stable Complex of Helium. *J. Phys. Chem. A* **2010**, *114*, 646–651. [CrossRef] [PubMed]
32. Khatua, M.; Pan, S.; Chattaraj, P.K. Confinement Induced Binding of Noble Gas Atoms. *J. Chem. Phys.* **2014**, *140*, 164306. [CrossRef] [PubMed]
33. Martínez-Guajardo, G.; Cabellos, J.L.; Díaz-Celaya, A.; Pan, S.; Islas, R.; Chattaraj, P.K.; Heine, T.; Merino, G. Dynamical Behavior of Borospherene: A Nanobubble. *Sci. Rep.* **2015**, *5*, 11287. [CrossRef]
34. Pan, S.; Ghara, M.; Kar, S.; Zarate, X.; Merino, G.; Chattaraj, P.K. Noble Gas Encapsulated B_{40} Cage. *Phys. Chem. Chem. Phys.* **2018**, *20*, 1953–1963. [CrossRef] [PubMed]
35. Stankevich, L.V.; Chistyakov, A.L.; Gal'pern, E.G. Polyhedral Boron Nitride Molecules. *Russ. Chem. Bull.* **1993**, *42*, 1634–1636. [CrossRef]
36. Xia, X.; Jelski, D.A.; Bowser, J.R.; George, T.F. MNDO Study of Boron-Nitrogen Analogues of Buckminsterfullerene. *J. Am. Chem. Soc.* **1992**, *114*, 6493–6496. [CrossRef]
37. Osawa, E. Superaromaticity. *Kagaku* **1970**, *25*, 854–863.
38. Reed, A.E.; Weinhold, F. Natural Bond Orbital Analysis of Near-Hartree–Fock Water Dimer. *J. Chem. Phys.* **1998**, *78*, 4066. [CrossRef]
39. Glendening, E.D.; Landis, C.R.; Weinhold, F. NBO 6.0: Natural Bond Orbital Analysis Program. *J. Comput. Chem.* **2013**, *34*, 1429–1437. [CrossRef]
40. Bader, R.F.W. *Atoms in Molecules a Quantum Theory*; Oxford University Press: Oxford, UK, 1990.
41. Morokuma, K. Why Do Molecules Interact? The Origin of Electron Donor-Acceptor Complexes, Hydrogen Bonding and Proton Affinity. *Acc. Chem. Res.* **1977**, *10*, 294–300. [CrossRef]
42. Ziegler, T.; Rauk, A. On the Calculation of Bonding Energies by the Hartree Fock Slater Method. *Theor. Chim. Acta* **1977**, *46*, 1–10. [CrossRef]
43. von Hopffgarten, M.; Frenking, G. Energy Decomposition Analysis. *Wiley Interdiscip. Rev. Comput. Mol. Sci.* **2012**, *2*, 43–62. [CrossRef]
44. Schlegel, H.B.; Millam, J.M.; Iyengar, S.S.; Voth, G.A.; Daniels, A.D.; Scuseria, G.E.; Frisch, M.J. Ab Initio Molecular Dynamics: Propagating the Density Matrix with Gaussian Orbitals. *J. Chem. Phys.* **2001**, *114*, 9758–9763. [CrossRef]
45. Iyengar, S.S.; Schlegel, H.B.; Millam, J.M.; Voth, G.A.; Scuseria, G.E.; Frisch, M.J. Ab Initio Molecular Dynamics: Propagating the Density Matrix with Gaussian Orbitals. II. Generalizations Based on Mass-Weighting, Idempotency, Energy Conservation and Choice of Initial Conditions. *J. Chem. Phys.* **2001**, *115*, 10291–10302. [CrossRef]
46. Schlegel, H.B.; Iyengar, S.S.; Li, X.; Millam, J.M.; Voth, G.A.; Scuseria, G.E.; Frisch, M.J. Ab Initio Molecular Dynamics: Propagating the Density Matrix with Gaussian Orbitals. III. Comparison with Born–Oppenheimer Dynamics. *J. Chem. Phys.* **2002**, *117*, 8694–8704. [CrossRef]
47. da Chai, J.; Head-Gordon, M. Long-Range Corrected Hybrid Density Functionals with Damped Atom–Atom Dispersion Corrections. *Phys. Chem. Chem. Phys.* **2008**, *10*, 6615–6620. [CrossRef] [PubMed]
48. McLean, A.D.; Chandler, G.S. Contracted Gaussian Basis Sets for Molecular Calculations. I. Second Row Atoms, Z = 11–18. *J. Chem. Phys.* **1980**, *72*, 5639–5648. [CrossRef]
49. Krishnan, R.; Binkley, J.S.; Seeger, R.; Pople, J.A. Self-consistent Molecular Orbital Methods. XX. A Basis Set for Correlated Wave Functions. *J. Chem. Phys.* **1980**, *72*, 650–654. [CrossRef]
50. Ditchfield, R.; Hehre, W.J.; Pople, J.A. Self-Consistent Molecular-Orbital Methods. IX. An Extended Gaussian-Type Basis for Molecular-Orbital Studies of Organic Molecules. *J. Chem. Phys.* **1971**, *54*, 724. [CrossRef]

51. Hehre, W.J.; Ditchfield, K.; Pople, J.A. Self—Consistent Molecular Orbital Methods. XII. Further Extensions of Gaussian—Type Basis Sets for Use in Molecular Orbital Studies of Organic Molecules. *J. Chem. Phys.* **1972**, *56*, 2257. [CrossRef]
52. Boys, S.F.; Bernardi, F.J.M.P. The calculation of small molecular interactions by the differences of separate total energies. Some procedures with reduced errors. *Mol. Phys.* **1970**, *19*, 553–566. [CrossRef]
53. Lu, T.; Chen, F. Multiwfn: A Multifunctional Wavefunction Analyzer. *J. Comput. Chem.* **2012**, *33*, 580–592. [CrossRef] [PubMed]
54. Baerends, E.J.; Ziegler, T.; Autschbach, J.; Bashford, D.; Bérces, A.; Bickelhaupt, F.M.; Bo, C.; Boerrigter, P.M.; Cavallo, L.; Chong, D.P.; et al. *ADF 2014.01*; SCM: Amsterdam, The Netherlands, 2014.
55. te Velde, G.; Bickelhaupt, F.M.; Baerends, E.J.; Fonseca Guerra, C.; van Gisbergen, S.J.A.; Snijders, J.G.; Ziegler, T. Chemistry with ADF. *J. Comput. Chem.* **2001**, *22*, 931–967. [CrossRef]
56. Frisch, M.J.; Trucks, G.W.; Schlegel, H.B.; Scuseria, G.E.; Robb, M.A.; Cheeseman, J.R.; Scalmani, G.; Barone, V.; Petersson, G.A.; Nakatsuji, H.; et al. *Gaussian 16, Rev. B.01*; Gaussian Inc.: Wallingford CT, USA, 2016.
57. Yin, D.; Yang, Y.; Yang, Y.; Fang, H. A Novel Fullerene-like $B_{30}N_{30}$ Structure: Stability and Electronic Property. *Carbon* **2016**, *102*, 273–278. [CrossRef]
58. Khatua, M.; Pan, S.; Chattaraj, P.K. Movement of Ng_2 Molecules Confined in a C_{60} Cage: An Ab Initio Molecular Dynamics Study. *Chem. Phys. Lett.* **2014**, *610–611*, 351–356. [CrossRef]
59. Ogilvie, J.F.; Wang, F.Y.H. Potential-Energy Functions of Diatomic Molecules of the Noble Gases I. Like Nuclear Species. *J. Mol. Struct.* **1992**, *273*, 277–290. [CrossRef]
60. Bader, R.F.W. A Bond Path: A Universal Indicator of Bonded Interactions. *J. Phys. Chem. A* **1998**, *102*, 7314–7323. [CrossRef]
61. Matta, C.F.; Hernández-Trujillo, J.; Tang, T.H.; Bader, R.F.W. Hydrogen–Hydrogen Bonding: A Stabilizing Interaction in Molecules and Crystals. *Chem. Eur. J.* **2003**, *9*, 1940–1951. [CrossRef]
62. Haaland, A.; Shorokhov, D.J.; Tverdova, N.V. Topological Analysis of Electron Densities: Is the Presence of an Atomic Interaction Line in an Equilibrium Geometry a Sufficient Condition for the Existence of a Chemical Bond? *Chem. Eur. J.* **2004**, *10*, 4416–4421. [CrossRef]
63. Bader, R.F.W.; Fang, D.C. Properties of Atoms in Molecules: Caged Atoms and the Ehrenfest Force. *J. Chem. Theory. Comput.* **2005**, *1*, 403–414. [CrossRef]
64. Poater, J.; Solà, M.; Bickelhaupt, F.M. Hydrogen–Hydrogen Bonding in Planar Biphenyl, Predicted by Atoms-In-Molecules Theory, Does Not Exist. *Chem. Eur. J.* **2006**, *12*, 2889–2895. [CrossRef] [PubMed]
65. Bader, R.F.W. Pauli Repulsions Exist Only in the Eye of the Beholder. *Chem. Eur. J.* **2006**, *12*, 2896–2901. [CrossRef] [PubMed]
66. Poater, J.; Solà, M.; Bickelhaupt, F.M. A Model of the Chemical Bond Must Be Rooted in Quantum Mechanics, Provide Insight, and Possess Predictive Power. *Chem. Eur. J.* **2006**, *12*, 2902–2905. [CrossRef] [PubMed]
67. Cremer, D.; Kraka, E. Chemical Bonds without Bonding Electron Density—Does the Difference Electron-Density Analysis Suffice for a Description of the Chemical Bond? *Angew. Chem. Int. Ed. Engl.* **1984**, *23*, 627–628. [CrossRef]
68. Pauling, L. The Formulas of Antimonic Acid and the Antimonates. *J. Am. Chem. Soc.* **1933**, *55*, 1895–1900. [CrossRef]
69. Ziółkowski, M.; Grabowski, S.J.; Leszczynski, J. Cooperativity in Hydrogen-Bonded Interactions: Ab Initio and "Atoms in Molecules" Analyses. *J. Phys. Chem. A* **2006**, *110*, 6514–6521. [CrossRef]
70. Pal, R.; Chattaraj, P.K. Possible Effects of Fluxionality of a Cavitand on Its Catalytic Activity through Confinement. *Phys. Chem. Chem. Phys.* **2021**, *23*, 15817–15834. [CrossRef]
71. Stone, A.J.; Wales, D.J. Theoretical Studies of Icosahedral C60 and Some Related Species. *Chem. Phys. Lett.* **1986**, *128*, 501–503. [CrossRef]